DYNAMIC MODEL OF A THERMAL SOLAR COLLECTOR

Agostino Gambarotta, Iacopo Vaja

University of Parma – Industrial Engineering Department
V. G.P. Usberti 181/A, 43100 Parma, Italy

vaja@ied.eng.unipr.it (Iacopo Vaja)

Abstract

In the paper a dynamic model for simulating the behavior of a thermal solar collector is presented. The collector is unglazed with a metal receiving pipe thermally linked to fins and presents thermal insulation in the back side and surface. The main characteristic of the proposed model is its capability of simulating the thermal performances for any given time discretization or collector axial discretization. The routine implemented is such to generate the system of partial differential equations (in matrix form) which dimension depends on the number of axial nodes assumed (n_x); the system is then numerically integrated upon the imposed discretization time (Δt). The model realized is *"White Box"* (all phenomena occurring within the component are studied referring to physical equations) and *"State Determined"* (state variables can be defined: energy storage is possible and heat can be accumulated both in the metal absorber and in the Heat Transfer Fluid).
The collector pipe is split up into n_x segments (axial discretization) with length Δx; for each of the segments energy conservation equations are applied to both the metal pipe and the Heat Transfer Fluid flowing within it. The component therefore presents a 2 node distribution in the longitudinal direction. The model is realized within Simulink® and is based on a Matlab® S-Function where all the equations are implemented in parameterized form and integrated.
Results of are proposed from dynamic simulations with different degrees of axial discretization of the system and with time varying inputs.

Keywords: Solar Collector, Dynamic model, Discretization, PDE integration

Presenting Author's biography

Iacopo Vaja received his Master Degree in Mechanical Engineering at University of Parma in 2004, after a thesis at ENEA (Italian National Agency for New Technologies, Energy and the Environment) where he worked at the R&D unit "Plant Control and Automation" of the "Solar Thermodynamic Project" – "Archimede Project". He is currently pursuing a Doctorate in Industrial Engineering at the University of Parma; the research activity is concerned to modeling and analysis of energy systems and networks for energy efficiency purposes.

ISBN 978-3-901608-32-2 *Copyright © 2007 EUROSIM / SLOSIM*

1 Introduction

In the paper a dynamic model of a thermal solar collector is presented.

Many steady state models have been proposed in literature. They have the advantage of simplicity, thus requiring low computing time, but, on the other hand, these in general lead to an overestimation of up to 10% of the energy delivered by the collector, as the thermal losses along the receiving pipe are not properly evaluated [1].

Other studies [2] propose three dimensional models of the thermal and hydro-dynamic fields during unsteady conditions, suitable for very detailed analysis of the flow and thermal distribution within the pipe and allowing for example to assess the effects of fins in the local parameters or the laminar mixed convection in the collector entrance region. These models appear indeed inadequate for overall thermal simulations of a solar system.

The model proposed allows assessing the behavior of a solar thermal collector under time varying mass flow rates of the heat transfer fluid (HTF) as well as the treatment of spatial non uniform solar radiation and heat transfer coefficients. The procedure is based on dividing the solar collector into n_x nodes along the axial direction and into 2 thermal nodes perpendicular to flow direction, resulting in $2 \times n_x$ partial differential equations [3]. Peculiarity of the procedure proposed is the possibility to define, through specific simulation parameters, both the degree of collector axial discretization and time discretization. This allows to define, by simply tuning the simulation parameters, very detailed thermal dynamic models as well as less detailed models of the collector (suitable for estimating overall thermal performances). Similar procedures, which also consider more than two longitudinal nodes, are proposed in [4,5] but the methods used to solve the model equations are not suitable for varying fluid mass flow rates.

The model of thermal solar collector will be integrated with models of other components within studies referring to Distributed Generation and Integrated Energy Systems. The simulation of the thermal behavior of a solar collector is an interesting issue as it implies the treatment of time-dependent weather conditions as well as time varying inlet fluid mass flow rates. This becomes important especially where these variables affect not only the dynamics within the collector but also of other energy systems if the solar thermal collector is integrated in a network where it is necessary to cover reliably the energy demand of a end user, residential or industrial.

A reliable precise and not too time consuming dynamic model of solar collector can be therefore a useful tool to study Integrated Energy Systems.

The aim of the work is also to develop a method of analysis and modeling of thermal energy systems which can be generalized not only to solar thermal collectors but also to other systems that implies heat exchanges under transient conditions. Particular attention will be paid upon the possibility to generalize the proposed procedure.

2 The system

The analyzed solar collector is of unglazed type and features a metal receiving pipe thermally linked to fins, in order to enhance solar heat absorption. Pipe and fins are of the same material and the model features a library with the physical properties (expressed as function of temperature) of different metals (such as copper and iron) in order allow considering different collector set ups. A scheme of a single pipe of the solar collector under analysis is proposed in Fig. 1, where the receiving pipe is perfectly connected to the fins at each side (no thermal resistance is assumed in the heat transfer between fins and pipe). This system can be considerd the basic element of a flat plate solar collector.

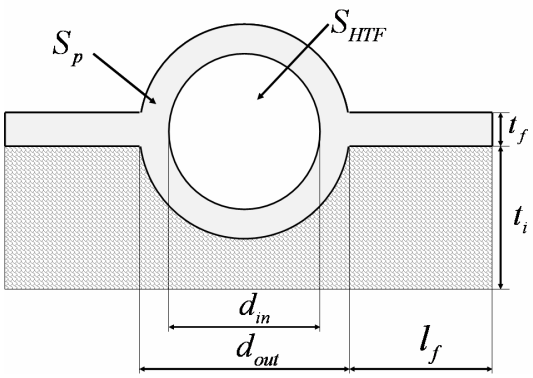

Fig. 1 Cross section of a pipe of the thermal solar collector

The collector has a thermal insulation in the back side. Properties of the insulation are not introduced in the model as the back side of the collector is considered ideally adiabatic. This means assuming the insulation to be ideal and that heat losses on the back side can be neglected compared to the heat losses in the upper side of the collector

Surface color of the external side may be considered for both the pipe and the fins, in order to reduce heat reirradiated from the collector and to enhance the absorption of the solar radiation. Properties of three different types of external paintings are loaded in the model, and their variation with temperature is considered: black paint, which may be used in the simplest collectors, Black Chrome and Cermet, if more advanced set ups are being modeled.

ISBN 978-3-901608-32-2

Copyright © 2007 EUROSIM / SLOSIM

The main heat fluxes within each pipe of the collector were defined as represented in the scheme of Fig. 2. The solar radiation upon the collector, q''_S, provides heat to the external side of the pipe and fins. Heat from the fins (q'_f) is transferred to the main pipe contributing to increase the heat flow to the HTF.

The increase in the pipe and fins temperature causes heat losses. These are mainly due to convection ($q'_{conv,f}$, $q'_{conv,p}$) with external air flowing upon the collector at wind speed u_w, and due to radiation ($q'_{rad,f}$, $q'_{rad,p}$); in this case heat is transferred from the collector to the sky, which is assumed at the sky temperature T_{sky}.

The balance among heat fluxes allows determining the net heat delivered to the heat transfer fluid ($q'_{conv,\ HTF}$), which is exchanged between the pipe internal side and the liquid mainly due to convection.

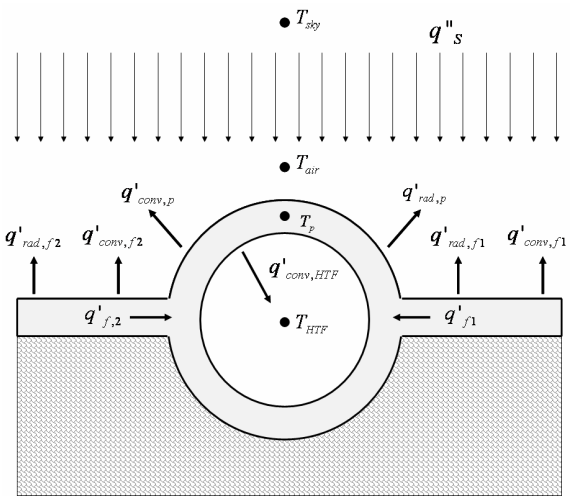

Fig. 2 Main heat fluxes and temperatures within the receiving pipe

3 Modeling the solar collector

In the present section a detailed description of the proposed model is provided. Some assumptions are first presented as well as a classification of the model.

The main equations are then introduced referring to a simple collector with only three axial volumes and the procedure is then generalized leading to the definition of the overall solving system in matrix form. The procedure of integration through finite difference method is then described.

The main equations used to describe the heat streams within each volume are also reported.

3.1 Model characteristics and assumptions

The model of the solar collector is assumed to be "State Determined", as it is possible to define state variables [6]. A State Determined model refers to a physical object where it is reasonable to assume a storage of mass, energy or momentum: such a component is considered therefore a "reservoir" according to its storage capabilities and state variables can be defined. In the case under analysis only energy storage is possible: heat can be accumulated both in the metal absorber and in the heat transfer fluid flowing within it.

A schematic representation of a State Determined model is provided in Fig. 3. It is characterized by a vector of time changing input variables $\bar{U}(t)$ and state variables $\bar{X}(t)$ while $\bar{Y}(t)$ is the vector of output variables. $\bar{U}(t)$ includes the vector of information variables $\bar{I}(t)$ from the plant control system.

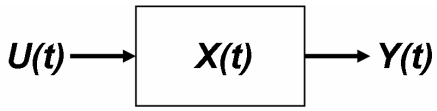

Fig. 3 Inputs, outputs and state variables of a State Determined component

A State Determined component can therefore be mathematically modeled by means of a system of equation that comprises differential equations (written in terms of the state variables) and algebraic equations (which bounds the other variables of the system to the state variables). A general form of this system of equation, in vector terms, is the following one:

$$\begin{cases} \dot{\bar{X}}(t) = f(\bar{X}(t), \bar{U}(t)) & \text{State Equation} \\ \bar{Y}(t) = g(\bar{X}(t), \bar{U}(t)) & \text{Output Equation} \end{cases} \quad (1)$$

In a State Determined system the outputs at time t depend not only on the inputs at the same instant t, but also on the state of the system at that instant t (Output Equation). The state of the system at t is a function of the inputs and of the time derivative of the state vector (State Equation): this latest differential equation represent the dynamics of the system. The State Equation needs in fact to be integrated in time in order to solve the output equation and to generate the output vector:

$$\bar{X}(t) - \bar{X}_0 = \int_{t_0}^{t} f\left(\bar{U}(t), \bar{X}(t)\right) dt \quad (2)$$

 Copyright © 2007 EUROSIM / SLOSIM

Eq. (2) shows how the output vector depends on the initial state of the system, $\overline{X}_0$ and on the "history" of the system, its evolution through time, mathematically represented by the time integral of the State Equation.

The collector pipe, which length is L, is split up into n_x segments (axial discretization) with length Δx. Each element defines a control volume according to the finite volume method of discretization. For each segment and at each instant of simulation t, energy conservation equations are applied to both the metal pipe (which local temperature is $T_p(t,x)$) and the heat transfer fluid flowing within it (which temperature is $T_{HTF}(t,x)$); the component therefore presents a 2 node distribution in the y direction. Temperatures at each equidistant node are calculated by the model and the value at an intermediate position may be determined by linear interpolation. A scheme of the generic pipe element is provided in Fig. 4, which refers to a longitudinal section of the receiving pipe, where the main heat fluxes are highlighted.

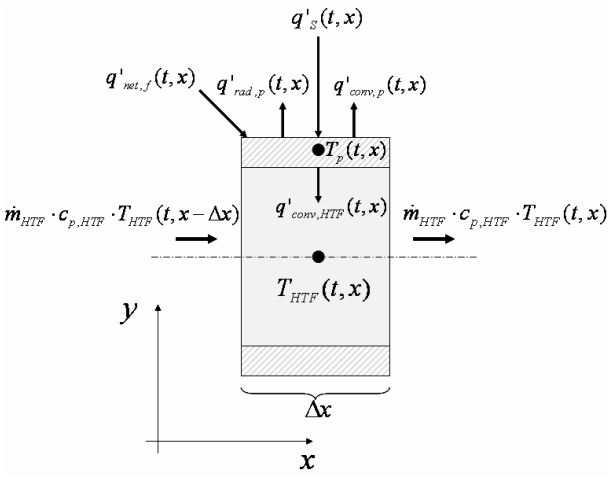

Fig. 4 Heat fluxes in a element of the receiving pipe

The state of the system is represented by the nodal temperature of both HTF and pipe at each instant of the simulation. Temperatures at the following time step can be obtained by integration of differential equation expressed in terms of derivative of the nodal temperatures, according to Eq. (2).

In Fig. 5 it is schematically proposed the block diagram of the model of solar collector with its input and outputs as well as the state variables.

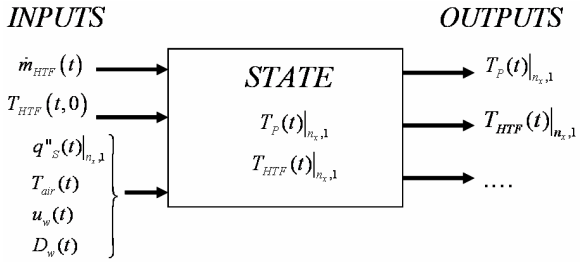

Fig. 5: Block diagram of the solar collector model

Inputs to the system at each time of simulation are represented by:

- heat transfer fluid mass flow rate through the collector ($\dot{m}_{HTF}(t)$);
- heat transfer fluid temperature at the collector inlet ($T_{HTF}(t,0)$);

Further inputs are represented by meteorological variables, which also influence the change in time of the state and output variables. These are assumed to be uncontrollable external inputs:

- solar radiation to the collector ($q''_S|_{n_x,1}(t)$), that is represented by a vector containing the actual value of the radiation upon each segment of the discretized collector (this allows considering spatial non uniform solar radiation and to study transient simulations such as cloud passing);
- air temperature ($T_{air}(t)$);
- wind speed ($u_w(t)$);
- wind direction, with respect to collector orientation ($D_w(t)$).

Several outputs can be generated by the model such as the local radiative or convective heat losses, the energy stored, etc. Among the model outputs, the system state variables (pipe and HTF nodal temperature) are certainly the most interesting to be taken into account, allowing to know not only the fluid output temperature but also the fluid and pipe temperature at each node and instant of simulation, helping to analyze the effects of varying input values on all the temperature distribution. These results could be hardly achieved by testing real components, where only the fluid output temperature is usually acquired. In this case therefore the output equation assumes the simplified form:

$$\overline{Y}(t) = \overline{X}(t) \tag{3}$$

It is possible to note that the size of both input and output vectors depend on the number of discrete volumes considered n_x; the length of the input vector is $5+n_x$ while the output vector is $2\times n_x$, in the

hypothesis of considering the nodal temperature of fluid and pipe as outputs.

The dimensions of the solving system of equations also depend on the number of nodes considered, as the overall number of state variables is, $2\times n_x$. A specific procedure is therefore created in order to allow this flexibility in the number of model inputs/outputs, as well as in the dimensions of the system of equations. The procedures are therefore implemented in Matlab® [7], in order to exploit its capabilities in matrix calculation, while the system graphical interface is realized within the Simulink® environment [8].

Simulink® is a software package for modeling, simulating, and analyzing dynamical systems. It is an icon based environment which supports linear and non-linear systems, modeled in continuous time, sampled time or a hybrid of the two. Simulink® includes a block library of sinks, sources, linear and non-linear components and connectors, allowing a hierarchical top-down and bottom-up modeling approaches. Its capabilities can be further improved by using S-function, which allow executing specific function written in C++®, Ada®, Fortan® or the Matlab® language while Simulink® is performing the simulation of a system, thus determining an equation based modeling approach. This peculiarity allows creating customized blocks with high degree of mathematical complexity, which would not be achieved when using only Simulink® custom blocks.

The model proposed is therefore based upon use of Matlab® S-Functions that allow writing State and Output equations in matrix and parameterized form, where the dimensions of the solving system and input/output vectors to the S-Function depend on the parameter n_x, that has to be defined before the simulation.

The proposed model of solar collector also features an internal solving procedure, instead of the embedded Simulink® solvers, based on the solution of a set of differential equations, written in terms of the derivative of the state variables with respect of time, according to a forward approach, thus providing a discrete state S-Function:

$$\frac{dX}{dt} = \frac{X_{t+\Delta t} - X_t}{\Delta t} \tag{4}$$

The following assumptions were made to generate the model:

- temperatures within the receiver (fluid, metal pipe and fins) are function of space and time;
- thermal capacitance of both the fluid and metal pipe are considered;
- the axial conductive heat flux is negligible [9];
- solar radiation is function of space and time;
- heat transfer due to conduction between pipe/HTF and pipe/air has been neglected;
- convective and radiation losses are considered only in the upper side of the collector, and the lower side is supposed perfectly insulated;
- the heat transfer fluid is liquid;
- thermodynamic properties of the HTF, the external air and metal pipe are function of the local node temperature;
- turbulent, transitional or laminar flow are considered to model convective heat transfer both in the HTF side and in the external air side of the pipe;
- the receiving pipe is considered to be as a single stretched pipe;
- metal pipe and fin temperature is assumed to be uniform at each node, according to the assumption of lumped thermal capacitance.

The hypothesis of lumped capacitance is quite stringent and not always valid: in order to be sure that the assumption is not cause of error, the Biot number is calculated both on the HTF and air side for each element of the pipe. The Biot number in fact provides a measure of the temperature drop in a solid exposed to convection, relative to the temperature difference between the surface and the fluid [10]. The dimensionless Biot number is defined as follows:

$$Bi = \frac{hL}{k} \tag{5}$$

If $Bi \ll 0.1$, it is reasonable to assume a uniform temperature distribution across the solid at any time during a transient process. This condition allows to assume that the resistance to conduction within the solid is much less that the resistance to convection across the fluid boundary layer, and hence the assumption of uniform temperature is reasonable. The Biot number therefore is calculated in the model for the solid system made up of the metal pipe and the side fins linked to it; whenever the condition $Bi \ll 0.1$ is not satisfied during simulation, the model stops and an error message is displayed.

The model realized can be considered as a “white box” as all phenomena occurring within the component are studied referring to physical equations, while the fact that many of these rely on empirical coefficients or correlations may allow to consider it as a “grey box”. In the following section a description of the main equations is provided as well as the methodology used in order to be able to consider a variable number of inputs and state variables of the system.

ISBN 978-3-901608-32-2 Copyright © 2007 EUROSIM / SLOSIM

3.2 The balance equations

For each control volume (Fig. 4) partial differential equations in discrete form may be written for the metal pipe and HTF respectively with proper boundary conditions, based on application of energy conservation. These equations have to be linked together in a system, depending on the number of volumes considered.

In Fig. 6 a very simple collector is considered where the longitudinal discretization is based on 3 elements only (n_x=3).

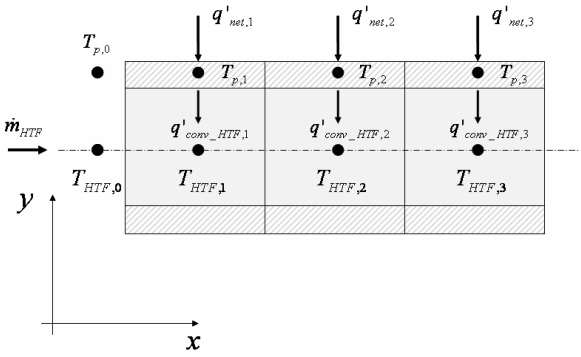

Fig. 6 Receiving pipe with three axial nodes

Energy balance at each node of the system leads to the following set of six ($2\times n_x$) equations:

$$\begin{cases} q'_{net,1} - q'_{conv\_HTF,1} = m_p c_{p_{p,1}} \dfrac{\partial T_{p,1}}{\partial t} \\ q'_{net,2} - q'_{conv\_HTF,2} = m_p c_{p_{p,2}} \dfrac{\partial T_{p,2}}{\partial t} \\ q'_{net,3} - q'_{conv\_HTF,3} = m_p c_{p_{p,3}} \dfrac{\partial T_{p,3}}{\partial t} \\ q'_{conv\_HTF,1} - \dot{m}_{HTF} c_{p_{HTF,1}} \left(T_{HTF,1} - T_{HTF,0}\right) = m_{HTF} c_{p_{HTF,1}} \dfrac{\partial T_{HTF,1}}{\partial t} \\ q'_{conv\_HTF,2} - \dot{m}_{HTF} c_{p_{HTF,2}} \left(T_{HTF,2} - T_{HTF,1}\right) = m_{HTF} c_{p_{HTF,2}} \dfrac{\partial T_{HTF,2}}{\partial t} \\ q'_{conv\_HTF,3} - \dot{m}_{HTF} c_{p_{HTF,3}} \left(T_{HTF,3} - T_{HTF,2}\right) = m_{HTF} c_{p_{HTF,3}} \dfrac{\partial T_{HTF,3}}{\partial t} \end{cases} \quad (6)$$

In the previous system of equations the different terms have the following meaning:

- q'_{net} is the heat exchanged between the pipe and the external environment. With reference to Fig. 4, for a generic element of the pipe at an axial abscissa *x*, is:

$$q'_{net}(x) = q'_{S}(x) + q'_{f}(x) - q'_{rad,p}(x) - q'_{conv,p}(x) \quad (7)$$

  where $q'_{f}(x)$ is the overall thermal contribution of the fins;

- $q'_{conv,HTF}$ is the heat exchanged between the pipe and the heat transfer fluid flowing within it. In steady state condition, at a generic axial node *x*, is:

$$q'_{conv,HTF}(x) = q'_{net}(x) \quad (8)$$

- m_p is the total mass of the pipe and its linked fins; for a discrete element of length Δx is:

$$m_p = \rho_{p,x} S_p c_{p_{p,x}} \Delta x \quad (9)$$

where S_p is the actual surface of the cross section of pipe and its linked fins (Fig. 1);

- m_{HTF} is the total mass of the fluid contained within each element of pipe; for a discrete element of length Δx is:

$$m_{HTF} = \rho_{HTF,x} S_{HTF} c_{p_{HTF,x}} \Delta x \quad (10)$$

where S_{HTF} is the pipe internal cross section (Fig. 1).

The system of equations (6) can be rearranged and written, in matrix form, as:

$$\left|\Phi\right|_{6,1} = \left|K\right|_{6,6} \cdot \left|\dot{T}\right|_{6,1} \quad (11)$$

Where Φ is the nodal thermal flux vector, K is the heat capacitance matrix and $\dot{T}$ is the vector containing the nodal temperature derivatives. Eq (11) represents the State Equation for the three nodes collector: at each time of simulation the state of the system is known and the only unknowns are the time derivatives of the state variables. It is possible to rewrite it according to the finite difference approach (Eq. 4) as follows:

$$\frac{\partial T_p}{\partial t} = \frac{T_p\big|_{t+\Delta t} - T_p\big|_t}{\Delta t} \quad (12)$$

$$\frac{\partial T_{HTF}}{\partial t} = \frac{T_{HTF}\big|_{t+\Delta t} - T_{HTF}\big|_t}{\Delta t} \quad (13)$$

Substituting the previous in Eq. (11) the only unknowns become the values of the state variables at the next step of simulation (time discrete simulation) which can be defined once a time interval Δt is defined (system parameter).

It is clear that the number of unknowns at each time steps is consistent with the number of balance equations written, and the system can be solved performing some matrix calculations, including matrix inversions.

The vector of unknowns for the simple collector with three axial nodes is provided below:

 Copyright © 2007 EUROSIM / SLOSIM

$$\begin{bmatrix} T_{p,1}\big|_{t+\Delta t} \\ T_{p,2}\big|_{t+\Delta t} \\ T_{p,3}\big|_{t+\Delta t} \\ T_{HTF,1}\big|_{t+\Delta t} \\ T_{HTF,2}\big|_{t+\Delta t} \\ T_{HTF,3}\big|_{t+\Delta t} \end{bmatrix} \tag{14}$$

The system of equations (6), obtained for a collector with only three nodes, can be rewritten for a generic solar collector where a higher number of nodes is defined. If n_x is the number of discrete elements, the system features a number of equations equal to the number of state variables, that are $2\times n_x$, with the following form:

$$\left|\Phi\right|_{2\cdot n_x,1} = \left|K\right|_{2\cdot n_x,2\cdot n_x} \cdot \left|\frac{T\big|_{t+\Delta t} - T\big|_t}{\Delta t}\right|_{2\cdot n_x,1} \tag{15}$$

In Fig. 7 a scheme of the way the model operates to set up the system of equations (15) and to solve it is reported.

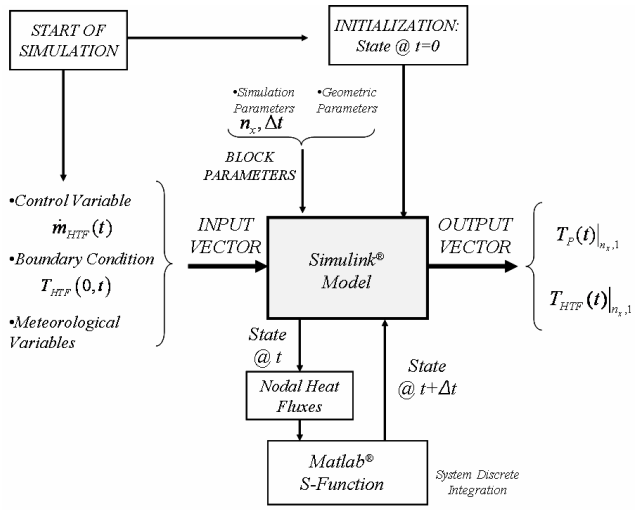

Fig. 7 Flow diagram of the main procedures of the model performed at each time step of simulation

The core of the system is the Simulink® model, which also represent the model graphical interface.

At start of simulation the system initialization procedure provides the system with the initial value of the state variables. The Simulink® block recalls at each time step of simulation the S-Function which also dialogs with external functions that perform the calculation of the thermal fluxes at each node; again this calculation is realized in matrix form. A detailed description of the equations used to determine the net value of the heat fluxes is given in the next section.

The Matlab® script compiled within the S-Function allows to define, at each time step of simulation, the system of equations (15). The procedure is parameterized with reference to the number of thermal nodes considered (n_x) which constitutes a parameterfor the Simulink® block in order to allow the simulation. Another block parameter is the discrete time step of integration Δt used by the discrete state S-function to perform the integration of the system and to calculate the state vector at the next time step. The internal procedure of numerical integration is able to operate regardless of the Simulink® solver integration time step. The S-Function therefore provides the Simulink® block with the value of the state variables at simulation time $t+\Delta t$.

The whole procedure is also influenced by the instantaneous value of the input variables, previously described. The HTF mass flow rate has been ticked in Fig. 7 as a control variable. In the physical system in fact a variation of the outputs (i.e. the fluid temperature at the collector outlet) is usually achieved by acting on the amount of fluid circulating within the collector, through proper fluid control devices (pumps or valves). This allows to respond to changes of the uncontrollable external inputs, such as the solar irradiation.

The model produces an output vector containing the temperatures of both the receiving pipe and the heat transfer fluid at each node of discretization.

Further parameters to be provided to the block are geometric data. These include pipe length (L), inner and outer diameter (d_{in}, d_{out}), fin length and thickness (l_f, t_f), pipe orientation, pipe material, type of selective absorber and type of heat transfer fluid.

These parameter, as well as the simulation parameters (n_x and Δt) are introduced through a block mask, shown in Fig. 8.

 Copyright © 2007 EUROSIM / SLOSIM

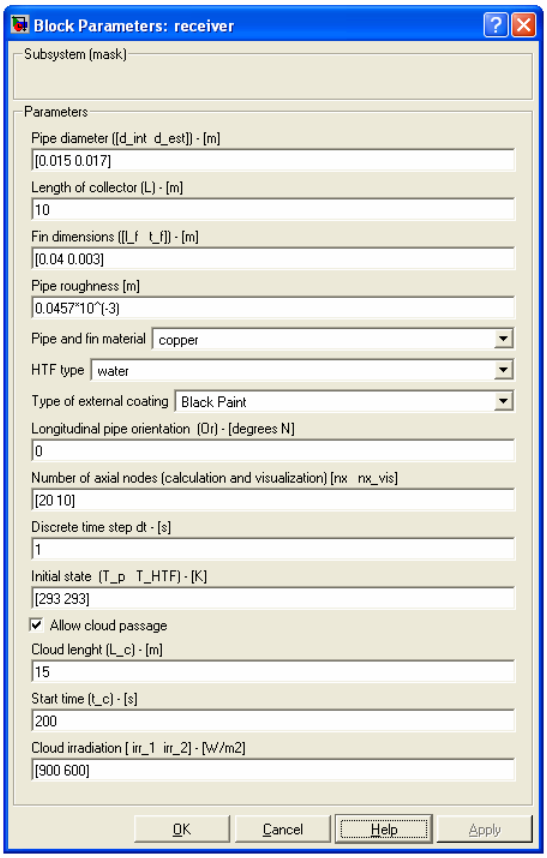

Fig. 8 Block dialog window of the Simulink® model of solar collector

3.3 Heat transfer equations

In the procedure proposed for the dynamic simulation of the solar collector, the Matlab® S-Funcion (where the system of partial differential equations is written and numerically integrated) calls external functions that perform the calculation of the heat fluxes, based on the instantaneous value of the HTF and pipe temperatures and on the value of the external inputs.

The effects of the local flow conditions are taken into account by calculating the local convection coefficients at each node on the basis of the local nodal temperature and the fluid flow conditions. Indeed the finest is the discretization the more acceptable is the approximation of assuming constant heat transfer coefficients over the discrete volume.

Values of heat fluxes are then provided to the S-Function in a proper format in order to allow placing the terms in the correct position within the main solving system of Eq. (15). Again the entire procedure of calculation of the heat fluxes is parameterized on the number of thermal nodes defined.

The heat transfer equations therefore are solved in matrix form in order to provide the main solving system with a vector of values consistent with the number of state variables.

The main equations used for heat transfer calculations have been obtained from literature [10-12] and are briefly described below for the receiving pipe.

- Convective heat transfer between pipe and heat transfer fluid:

$$q'_{conv,HTF} = h_{HTF}\left(T_p - T_{HTF}\right) \qquad (16)$$

where the convection heat transfer coefficient can be determined from the dimensionless Nusselt number:

$$Nu = \frac{h_{HTF} D}{k_{HTF}} \qquad (17)$$

At each node the Nusselt number is calculated depending on whether the flow is laminar or not: in case of laminar flow Nu=4.36 while in case of transitional and turbulent flow regime (Re>2300) Nusselt number can be determined from the Gnielinsky correlation:

$$Nu_{HTF} = \frac{(f/8)(\mathrm{Re}-1000)\,\mathrm{Pr}_{HTF}}{1+12.7\sqrt{f/8}\left(\mathrm{Pr}_{HTF}^{\,2/3}-1\right)} \qquad (18)$$

where f is the friction factor.

- Convective heat transfer between pipe and external air:

$$q'_{conv,p} = \bar{h}_{air} x\left(T_p - T_{air}\right) \qquad (19)$$

The profile of the pipe has been assumed as a flat slab in case of longitudinal air stream and the properties are calculated at film temperature.

The local convection heat transfer coefficient can be determined from the local Nusselt number:

$$Nu_x = \frac{h_x x}{k_{air}} \qquad (20)$$

Once again at each node the Reynolds number is calculated and the Nusselt number is determined depending on the flow conditions.

In case of laminar flow:

$$Nu_x = 0.332\,\mathrm{Re}_x\,\mathrm{Pr}^{1/3} \quad \mathrm{Pr} > 0.6 \qquad (21)$$

In case of turbulent flow:

$$Nu_x = 0.0296\,\mathrm{Re}_x^{\,4/5}\,\mathrm{Pr}^{1/3} \quad 0.6 < \mathrm{Pr} < 60 \qquad (22)$$

- The radiative losses are calculated for long concentric cylinders under the hypothesis of radius of external cylinder being much bigger than internal cylinder.

 Copyright © 2007 EUROSIM / SLOSIM

$$q_{rad} = \varepsilon_p \sigma \pi \frac{d_{out}}{2}\left(T_p{}^4 - T_{sky}{}^4\right) \qquad (23)$$

The external cylinder, which receives heat through radiation from the collector pipe, is the sky, and the sky temperature has to be calculated:

$$T_{sky} = -100.4 + 1.269 T_{air} \qquad (24)$$

- The net heat from finned surfaces measures the actual heat that contributes heating the receiving pipe and in turns the heat transfer fluid.

For each fin placed aside the receiving pipe, the following correlation may be written:

$$q'_{f1} = q'_S - q'_{conv,f} - q'_{rad,f} \qquad (25)$$

The different terms that appear in the previous equation can be calculated according to correlations analogous to those proposed for the receiving pipe. The heat transfer equations are defined assuming a fin temperature equal to the pipe temperature, which is consistent with the hypothesis of lumped capacitance for the pipe and fins body (i.e. no heat resistance to conduction has been assumed between fin and pipe).

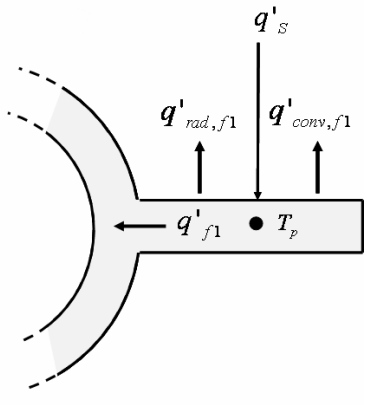

Fig. 9 Heat fluxes in the fins

4 Model validation

To assess the validity of the proposed model the results of some simulations have been compared to data gathered from a test facility where a real solar collector have been tested.

These data derive from literature: in a study by Tripanagnostopoulos et. al. [13] experimental results from testing of three flat plate solar collectors with black, blue red and brown absorber, with and without glazing are presented. The purpose of the study was to compare the different types of external coloring and for different collector types, in order to evaluate experimentally the effect of differently colored absorbers on the collector efficiency. One of the collectors tested has geometric characteristics compatible with the presented model. Such collector is unglazed with back insulation, made with copper pipes with 0.01m internal diameter and 0.012m external diameter, placed parallel at a distance 0.08m each other and in thermal contact with a thin copper fin. The collector has been colored externally with black paint.

The collector described was purposely constructed for the experiment and was tested outdoors, in steady state operating conditions during noon, with variable input water temperature while the water mass flow rate was fixed to 0.02kg/s. Thermocouples were used to measure input and output temperatures, as well as some intermediate temperatures. Solar radiation intensity at the collector plane and wind speed were also measured during the experiment. Solar irradiation q''_S was always greater than 800W/m^2 and wind speed u_W was below 2m/s.

From the data recorded graphs have been created for each type of collector were the collector steady state efficiency ($\eta_C = \frac{\dot{m}_{HTF} c_{P_{HTF}} \left(T_{out} - T_{in}\right)}{q''_S S_C}$) has been plotted as function of the ratio $\frac{\Delta T}{q''_S} = \frac{\left(T_{in} - T_{air}\right)}{q''_S}$. The collector efficiency measures the amount of the solar energy to the collector effectively transferred to the fluid.

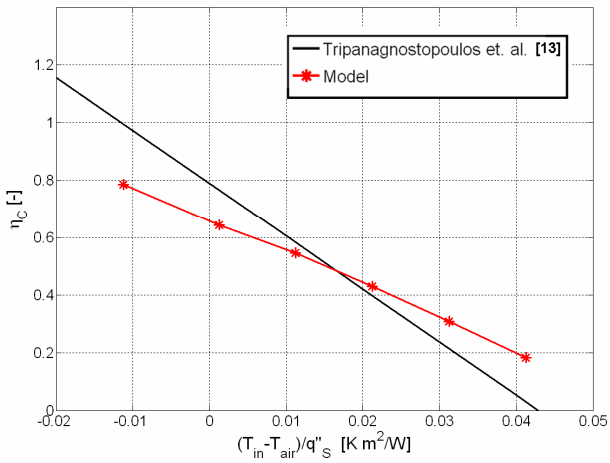

Fig. 10 Steady state efficiency results of the tested collector and the model

The geometric parameters of the real collector described in [13] have been introduced into the model, black paint has been considered for external collector coloring and the same inputs as the real system have been considered for the simulation (meteorological data and fluid mass flow rate). A set of simulations

 Copyright © 2007 EUROSIM / SLOSIM

have been performed with different water inlet temperatures and the steady state model outputs have been used to calculate the collector efficiency. Values obtained from the model have been plotted in the graph of Fig. 10 which also reports the curve of the measured data.

To assess the accuracy of the model with respect to the result from the real collector, the actual model output were compared with the output of the real system. Model output (the fluid temperature at collector outlet) was compared with the fluid temperature leaving the real collector. The error ($\varepsilon_{abs} = T_{out}\big|_{\exp} - T_{out}\big|_{\mathrm{mod}}$) is displayed in Fig. 11 a): it can be observed that an absolute error of only few degrees Kelvin in the fluid temperature exists between the experimental data and results from the model:

In Fig. 11 b) the relative error is plotted, as:

$$\varepsilon = \frac{T_{out}\big|_{\exp} - T_{out}\big|_{\mathrm{mod}}}{T_{out}\big|_{\exp}} \cdot 100 \qquad (26)$$

The agreement between the results from the model and the data from the experimental facility appears good, confirming that the correlations used to describe the main heat transfer phenomena occurring within the collector are appropriate. It also demonstrates the validity of the method used to create and solve the system of equations, at least in steady state conditions. Unfortunately a validation of the behavior of the model under unsteady condition has not been possible so far for the lack of experimental data.

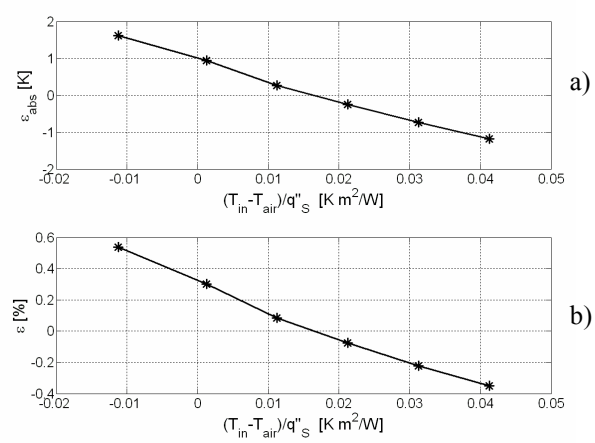

Fig. 11 Absolute error (a) and relative error (b) between fluid outlet temperature measured from experimental setup and calculated from the model

5 Simulations

Following the described validation, some simulations have been performed with the model proposed. Among the several inputs that may affect the behavior of the system indeed the HTF mass flow rate circulating through the collector and the net solar irradiation are those that have major effects in determining changes in the fluid outlet temperature, which represent the main output variable. Results of two simulations are therefore proposed in this section.

In the first simulation a step change in the fluid mass flow rate is imposed. At simulation time t=2000s the mass flow rate circulating within the receiving pipe suddenly decreases from the initial value of 0.025kg/s to 0.015kg/s, as shown in Fig. 12 a). In this case the solar radiation has been assumed to be uniform and equal to 1000W/m^2.

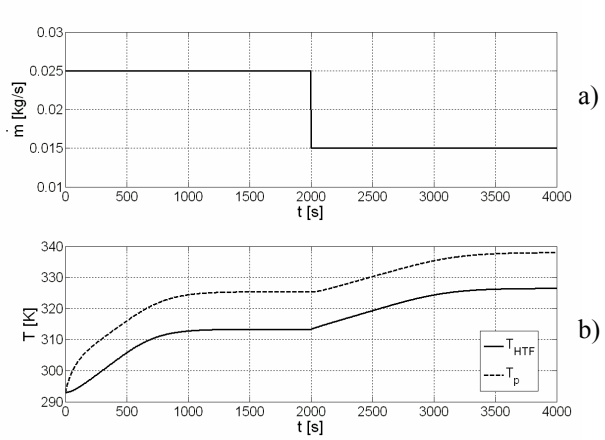

Fig. 12 a) Step change in the HTF mass flow rate – b) Response in the HTF and pipe temperature in the outlet receiver section

The collector under analysis is characterized by a 20m long copper receiving pipe with high performance black-chrome selective absorber; the heat transfer fluid is water.

As initial condition (model initialization) it is assumed collector and HTF temperature equal to 293K; as boundary condition the HTF temperature at the receiver inlet section is set again at 293K during the whole duration of simulation.

The model has been simulated referring to an axial discretization Δx=2m (n_x=10) and a time discretization Δt=5s (simulation parameters).

The response of the system to the step change in the fluid mass flow rate is shown in Fig. 12 b), where the temperature of the fluid, as well as of the receiving pipe, are plotted with respect to time: both temperatures refer to the outlet section of the receiver. It can be observed that, starting from the same temperature for both pipe and HTF at t=0s (model initialization), a sudden increase in the pipe temperature allows the HTF temperature to rise, but at a slower rate. Steady state conditions are reached after about 1000s of simulation. When the step change in the HTF mass flow rate circulating within the pipe is imposed, a new transient condition in the fluid and pipe temperature can be observed; the reduced mass

that circulates within the receiver allows a further rise in the temperatures.

The procedure that has been created for simulating the thermal behavior of the solar collector allows creating more complete representations of the temperature distribution within the system and three dimensional graphs can be plotted which allow to evaluate the temperature distribution for each cross section of the pipe according to the axial discretization imposed. The model in fact returns the values of HTF and pipe temperature not only in the outlet section of the receiver but also for each axial node.

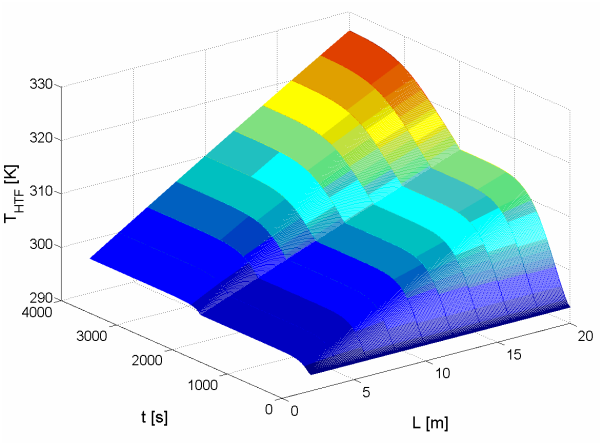

Fig 13 Heat transfer fluid temperature distribution due to a step change in the HTF mass flow rate

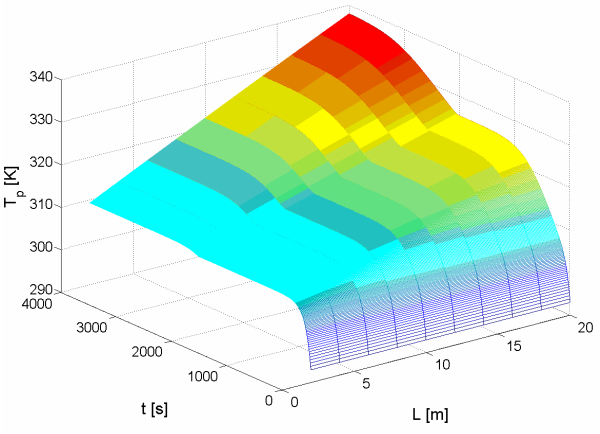

Fig. 14 Pipe wall temperature distribution due to a step change in the HTF mass flow rate

In Fig. 13 the fluid temperature is plotted with respect to time of simulation and collector length. It can be observed that the temperature profile at the outlet section (at L=20m from inlet) corresponds to that shown in Fig. 12 b), which in fact may be considered as a section of the three-dimensional plot of Fig. 13. It can also be noticed how the temperature profile in the first node (at a distance L=2m from inlet) is almost flat and close to the water entering temperature set to 293K.

An analogous pattern of the temperatures, with respect to time of simulation and receiver length, is proposed in Fig. 14 for the pipe.

In the second set of results here presented, which refer to the same collector described above, the heat transfer fluid mass flow rate has been assumed to be constant and equal to 0.02kg/s, while a variation with time in the solar radiation has been considered (Figg. 15-17).

The results reported allow to assess the effects on the fluid and pipe temperatures due to a cloud passage, imposed at simulation time t=250s, which determines a sharp decrease in the solar radiation to the collector, as shown in Fig. 15 where net solar radiation is plotted with respect to time of simulation and collector length. Cloud shade is assumed to be 15m long and with a speed of 0.5m/s: the solar irradiation at clear sky condition is assumed 1100W/m^2 and the value decreases to 300W/m^2 when cloud is passing. The cloud moves longitudinally along the collector (under the hypothesis that the receiving pipe does not make bends) and it starts shading the receiver from the inlet. It is possible to observe that at each point along the pipe the reduction in the solar radiation (as well as the subsequent increase to the original value) occur at a time that is proportional to the distance from collector inlet. A special procedure for evaluating cloud passing upon the collector has been set up and cloud parameters can be introduced in the Simulink® block dialog window (Fig. 8).

The three dimensional graphs allow in this case to appreciate the temperature distribution of both fluid and pipe with respect to time and space, due to the non uniform solar radiation caused by the cloud: the HTF temperature is plotted as function of time and distance from pipe inlet in Fig. 16 while the pipe wall temperature is reported in Fig. 17.

The results have also been proposed in this case with two different sets of the simulation parameters, in order to demonstrate how different degrees of discretization may be considered for the same physical system, depending on the accuracy required.

In Figg. 16 a) and 17 a) a spatial discretization of Δx=4m was assumed (n_x=5, thus the solving system features 10 equations) with a time discretization Δt=50s. The computational time required for the simulation of such system is 3.2s on a Pentium® IV desktop computer.

A finer simulation is proposed in Figg. 16 b) and 17 b) were Δx is 0.5m (then n_x=40, with 80 equations to be solved at each time step of simulation) and Δt=1s; the time required for simulation in this case is 19.5s.

ISBN 978-3-901608-32-2

Copyright © 2007 EUROSIM / SLOSIM

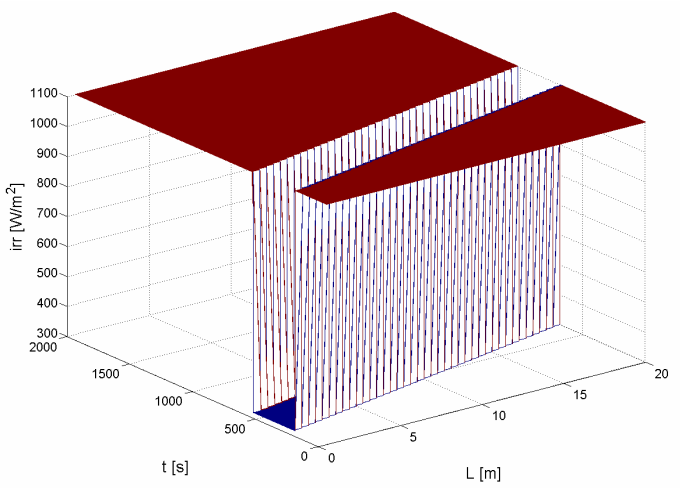

Fig. 15 Solar radiation to the collector due to cloud passage

a) b)

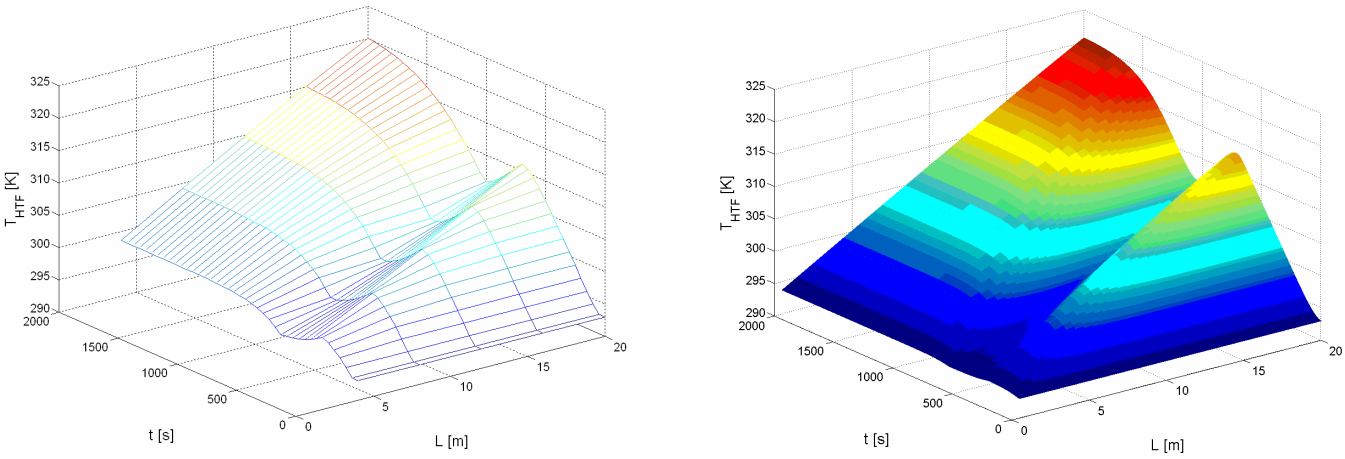

Fig. 16 Heat transfer fluid temperature distribution during cloud passage with two different degrees of spatial and time discretization

a) b)

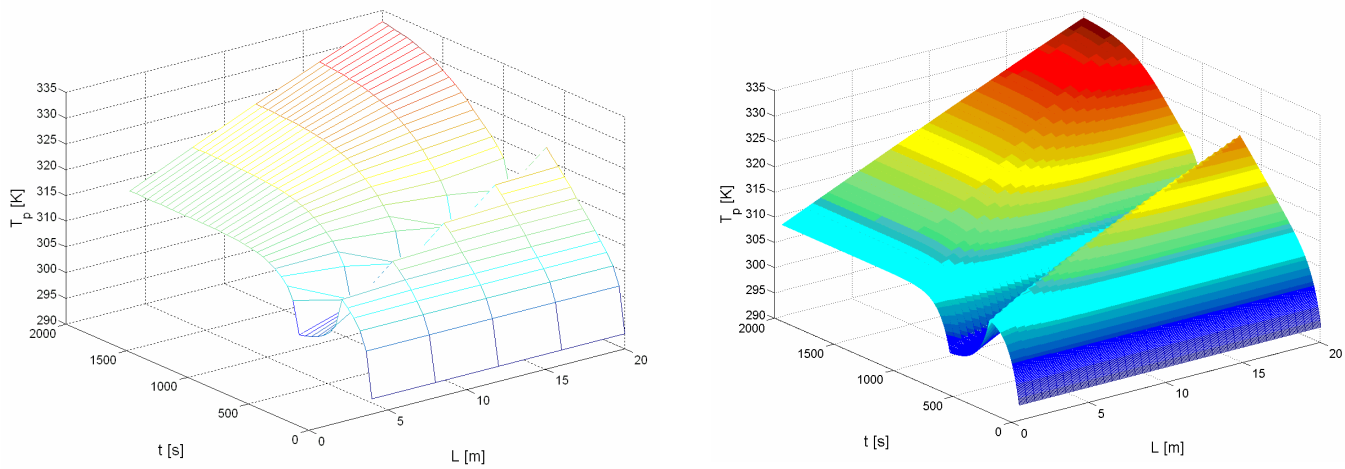

Fig. 17 Pipe wall temperature distribution during cloud passage with two different degrees of spatial and time discretization

The results of simulation shown in Figg. 16 a) and 16 b), for the same physical system but with different spatial and time discretization, have been compared. The plot of Fig. 18 has been obtained as the difference of the value of the HTF temperature calculated with the two different sets of simulation parameters, for each corresponding combination of simulation time t and distance from collector inlet L. ΔT_{HTF}, reported in the z-axis of Fig. 18, is the difference between the fluid temperature calculated through the rough discretization (n_x=5, Δt=50s) and the temperature calculated with the fine discretization (n_x=40 Δt=1s).

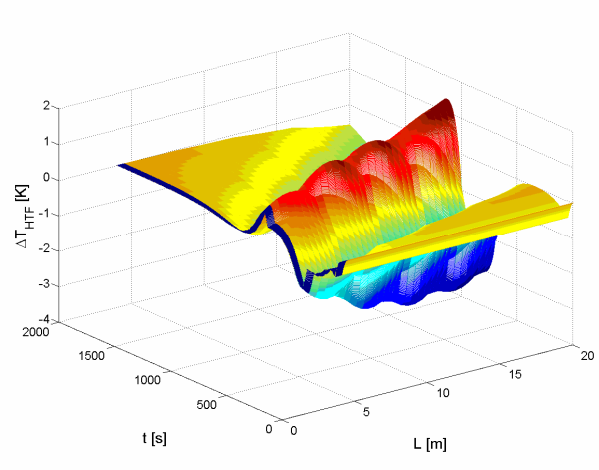

Fig. 18 Difference in the HTF temperature calculated with two different degrees of spatial and time discretization

It can be observed that differences exist between the results obtained with the two sets of simulation parameters. During the transient condition caused by the cloud passing, the rough model lags a little in calculating the decrease in HTF temperature. The opposite occurs when the cloud uncovers the collector and the fine model is quicker in demonstrating the increase in the fluid temperature. This effect is certainly due to the higher time step assumed for the rough model (50 s instead than 1 s), but also the spatial discretization has some implications: the temperature difference is however contained within few degrees Kelvin.

It can also be noticed from Fig. 18 that the steady state values of the HTF temperature calculated with the two different degrees of discretization do not show significant difference and both models provide the same steady state fluid temperature.

For general applications of the model, roughest discretization degrees may therefore be accepted, also considering the much lower computational time required when the number of axial nodes is reduced and time interval is increased. Whenever precise description of transient phenomena is required, the model can provide much higher calculation performances of the same physical system, by simply tuning the simulation parameters through the block dialog mask.

6 Conclusions

The analytical procedure used to create a flexible dynamic model of a thermal solar collector has been presented in the paper. The computational method allows great flexibility as it is possible generate very detailed thermal dynamic models as well as roughest models that are still able to describe the dynamic behavior of the system. The degree of precision required can be simply tuned through a user friendly block parameter mask. The fully parameterized procedure, written to calculate the heat fluxes at each node and to set up the system of partial differential equations, is based on matrix calculations and allows the user to act on the simulation only by varying the model inputs, once the parameters have been introduced.

Some dynamic simulations have been proposed and change in fluid and pipe temperatures are shown under changing input conditions.

The model has also been validated under steady state conditions by comparing the results of simulations with experimental data gathered from testing of a real solar collector: the agreement appears good, confirming the validity of the method adopted.

Computational time of the model is very interesting, also in case of more detailed simulations. In general rough simulations (small degree of axial discretization, high time step intervals) seem to be acceptable for general purpose application of the solar collector. The simulation time in this case is almost 1000 times faster than real time.

The procedure proposed will be adopted also for simulating other thermal systems which involve heat exchange, such as heat recovery boilers used within cogenerating systems or for the simulation of district heating networks.

ISBN 978-3-901608-32-2

Copyright © 2007 EUROSIM / SLOSIM

7 Nomenclature

c_p	*Specific heat at constant pressure[J/kg K]*
d	*Diameter [m]*
f	*Friction factor [-]*
h	*Convection heat transfer coefficient [W/m^{2}K]*
k	*Thermal conductivity [W/mK]*
m	*Mass [kg]*
$\dot{m}$	*Mass flow rate [kg/s]*
q'	*Heat transfer rate per unit length [W/m]*
q''	*Heat Flux [W/m^2]*
t	*Time [s] - Thickness [m]*
u	*Speed [m/s]*
Bi	*Biot number [-]*
L	*Length [m]*
Nu	*Nusselt number [-]*
Pr	*Prandtl number [-]*
Re	*Reynolds number [-]*
S	*Surface area [m^2]*
T	*Temperature [K]*

Greek Letters

ε	*Emissivity[-], Relative error [-]*
σ	*Stefan-Boltzmann constant [-]*
η	*Efficiency [-]*

Subscripts

abs	*Absolute*
cond	*Conduction*
conv	*Convection*
exp	*Experimental*
f	*Fin*
i	*Insulation*
irr	*Irradiation*
in	*Inner*
mod	*Model*
o	*Outer*
p	*Pipe*
rad	*Radiative*
x	*Axial abscissa*
y	*Longitudinal abscissa*
w	*Wind*
C	*Collector*
HTF	*Heat Transfer Fluid*
S	*Sun*

8 References

[1] J. Schnieders. Comparison of the energy yield prediction of stationary and dynamic solar collector models and the model's accuracy in the description of a vacuum tube collector. *Solar Energy*, 61:179-190, 1997.

[2] M. Ouzzane, N. Galanis. Numerical analysis of mixed convection in inclined tubes with external longitudinal fins. *Solar Energy*, 71:199-211, 2001.

[3] F. Hilmer, K. Vajen, A. Ratka, H. Ackermann, W. Fuhs, O. Melsheimer. Numerical solution and validation of a dynamic model of solar collectors working with varying fluid flow rate. *Solar Energy*, 65:305-321, 1999.

[4] W. Kamminga. The approximate temperatures within a flat-plate solar collector under transient conditions. *International Journal of Heat and Mass Transfer*, 28:433-440, 1985.

[5] A. J. de Ron. Dynamic Modelling and verification of a flat plate solar collector. *Solar Energy*, 24:117-128, 1980.

[6] L. Guzzella, C. H. Onder. Introduction to Modeling and Control of Internal Combustion Engine Systems. Springer Verlag. 2004.

[7] Matworks. *MATLAB User's guide*. The Matworks Inc., Natick, 1990.

[8] Matworks. *SIMULINK User's guide*. The Matworks Inc., Natick, 1990.

[9] P.R. Prabhankar. Two dimensional configuration analysis of a flat plate solar collector. Ph. D. thesis in Mechanical Engineering, University of Oklahoma, USA, 1975.

[10] F.P Incroprera, D.P De Witt. Fundamentals of Heat and Mass Transfer. John Wiley & Sons. 2001.

[11] G.N. Tiwari. Solar Energy – Fundamentals, Design, Modelling and Applications. Alpha Science International. 2002.

[12] C. Oliveti, N. Arcuri, S. Ruffolo. Un modello orario della radiazione infrarossa atmosferica per giornate serene. 55° congresso ATI – Bari 2000.

[13] Y. Tripanagnostopoulos, M. Soulitis, T. Nousia. Solar Collectors with colored absorbers. *Solar Energy*. 68:343-356, 2000.

ISBN 978-3-901608-32-2 Copyright © 2007 EUROSIM / SLOSIM